AGU PUBLICATIONS

Geophysical Research Letters

RESEARCH LETTER
10.1002/2017GL076721

Key Points:
- The shape of the aerosol size distribution is a key factor for the sensitivity of homogeneous ice nucleation to aerosol perturbations
- This study reconciles the large discrepancy in aerosol sensitivity of ice numbers in previous studies on homogeneous ice nucleation
- Different aerosol sensitivities in homogeneous ice nucleation parameterizations result in an aerosol LW indirect forcing between 0.05 and 0.36 W m^{-2}

Correspondence to:
X. Liu,
xliu6@uwyo.edu

Citation:
Liu, X., & Shi, X. (2018). Sensitivity of homogeneous ice nucleation to aerosol perturbations and its implications for aerosol indirect effects through cirrus clouds. *Geophysical Research Letters*, *45*, 1684–1691. https://doi.org/10.1002/2017GL076721

Received 7 DEC 2017
Accepted 25 JAN 2018
Accepted article online 29 JAN 2018
Published online 12 FEB 2018

©2018. American Geophysical Union. All Rights Reserved.

Sensitivity of Homogeneous Ice Nucleation to Aerosol Perturbations and Its Implications for Aerosol Indirect Effects Through Cirrus Clouds

X. Liu[1] and **X. Shi**[1,2]

[1]Department of Atmospheric Science, University of Wyoming, Laramie, WY, USA, [2]School of Atmospheric Sciences, Nanjing University of Information Science and Technology, Nanjing, China

Abstract The magnitude and sign of anthropogenic aerosol impacts on cirrus clouds through ice nucleation are still very uncertain. In this study, aerosol sensitivity (η_α), defined as the sensitivity of the number concentration (N_i) of ice crystals formed from homogeneous ice nucleation to aerosol number concentration (N_a), is examined based on simulations from a cloud parcel model. The model represents the fundamental process of ice crystal formation that results from homogeneous nucleation. We find that the geometric dispersion (σ) of the aerosol size distribution used in the model is a key factor for η_α. For a monodisperse size distribution, η_α is close to zero in vertical updrafts ($V < 50$ cm s^{-1}) typical of cirrus clouds. However, η_α increases to 0.1–0.3 (i.e., N_i increases by a factor of 1.3–2.0 for a tenfold increase in N_a) if aerosol particles follow lognormal size distributions with a σ of 1.6–2.3 in the upper troposphere. By varying the input aerosol and environmental parameters, our model reproduces a large range of η_α values derived from homogeneous ice nucleation parameterizations widely used in global climate models (GCMs). The differences in η_α from these parameterizations can translate into a range of anthropogenic aerosol longwave indirect forcings through cirrus clouds from 0.05 to 0.36 W m^{-2} with a GCM. Our study suggests that a larger η_α (0.1–0.3) is more plausible and the homogeneous nucleation parameterizations should include a realistic aerosol size distribution to accurately quantify anthropogenic aerosol indirect effects.

1. Introduction

The sensitivity of cloud properties to aerosol perturbations is critical for the estimation of anthropogenic aerosol radiative forcing and thus the projection of future climate change (Boucher et al., 2013). Compared to warm clouds, anthropogenic aerosol indirect forcing (AIF) through cirrus clouds is controversial and associated with large uncertainties (Barahona & Nenes, 2011; Fan et al., 2016; Liu et al., 2009; Wang et al., 2014). Ice formation in cirrus clouds can result from the homogeneous freezing of aerosol solution particles (e.g., sulfate) and the heterogeneous freezing of insoluble or partially insoluble aerosol particles (e.g., mineral dust) (Barahona & Nenes, 2009; Kärcher et al., 2006; Pruppacher & Klett, 1997). The details of homogeneous and heterogeneous freezing processes, as well as their relative contributions to cirrus cloud formation in the upper troposphere, are still poorly understood (Cziczo et al., 2013; DeMott et al., 2003; Jensen et al., 2013; Murray et al., 2010). This poor understanding leads to a large uncertainty in the parameterizations of ice nucleation for global climate models (GCMs) (Barahona et al., 2014; Kuebbeler et al., 2014; Liu, Shi, et al., 2012; Zhang et al., 2013).

Anthropogenic aerosols, such as sulfate, have increased substantially from the preindustrial (PI) era to the present day (PD) (Lohmann & Feichter, 2005). For a fixed liquid water content in warm clouds, an increase in aerosol concentrations leads to a larger number of small cloud droplets, which increases the solar reflectivity of clouds (Twomey, 1977). On the other hand, it is not determined whether an increase in the upper tropospheric sulfate aerosol concentration (N_a [cm^{-3}]) leads to an appreciable increase in the number concentration of ice crystals (N_i [cm^{-3}]) by homogeneous freezing in cirrus clouds. Some studies based on cloud parcel model simulations showed that N_i is nearly invariant to N_a with updrafts lower than approximately 50 cm s^{-1} (Kärcher & Lohmann, 2002a, 2002b; Kay & Wood, 2008). However, other modeling studies showed that N_i is more sensitive to N_a (Barahona & Nenes, 2008; Jensen & Toon, 1994; Liu & Penner, 2005). For example, these authors found that for a variation in N_a by a factor of 10, N_i varies by a factor of 1.5 to 3, depending on the updraft (i.e., cooling rate) and temperature. Correspondingly, the Community Atmosphere Model version 5.1 (CAM5.1), with the Liu and Penner (2005) parameterization, simulates a stronger longwave AIF

Table 1
Parcel Model Sensitivity Experiments Conducted in This Study

Experiment	Configuration
RAD0.02	T = 220 K, P = 250 hPa, and α_i = 0.1. Aerosol size is monodispersed, where R_a = 0.02 μm.
SIGMA1.6	Same as RAD0.02 but aerosols follow a lognormal size distribution with R_a = 0.02 μm and σ = 1.6.
SIGMA2.3	Same as SIGMA1.6 but σ = 2.3.
RAD0.2	Same as RAD0.02 but R_a = 0.2 μm.
ALFA0.5	Same as SIGMA1.6 but α_i = 0.5.
ALFA0.5_KL	Same as ALFA0.5 but homogeneous freezing is calculated based on the concept of the KL parameterization.

Note. KL = Kärcher et al. (2006).

(0.40–0.52 W m^{-2}) (Ghan et al., 2012) than the ECHAM-HAM2 model (0.05–0.2 W m^{-2}) (Zhang et al., 2012) by using the Kärcher and Lohmann (2002a, 2002b) parameterization.

Following Kay and Wood (2008), an aerosol sensitivity parameter, η_α, is defined as

$$\eta_\alpha = \frac{d(\ln N_i)}{d(\ln N_a)} \tag{1}$$

$\eta_\alpha \ll 1$ implies that the aerosol has a negligible effect on N_i, and the anthropogenic AIF through cirrus clouds is rather weak, while a larger η_α indicates an appreciable aerosol effect and a stronger anthropogenic AIF. Here we focus on the homogeneous nucleation of sulfate solution particles in this study. We first use a cloud parcel model to investigate the sensitivity of N_i to N_a (i.e., the magnitude of η_α) and the controlling parameters for η_α. Then, we discuss the difference in η_α among three physically based ice nucleation parameterizations developed by Liu and Penner (2005) (LP), Barahona and Nenes (2009) (BN), and Kärcher et al. (2006) (KL). We are able to explain the reasons for large η_α differences among these three parameterizations. Finally, the implications of the η_α difference for AIF through cirrus clouds are quantified using CAM5.1.

2. Determining Factors of η_α

Ice formation through homogeneous nucleation in cirrus clouds can be modeled by solving the theoretical formulations that describe the primary formation of ice crystals in an adiabatically rising air parcel. Usually, physically based ice nucleation parameterizations are developed based on (or validated against) cloud parcel model simulations. Here we study η_α using a cloud parcel model (Shi & Liu, 2016) and turn off the heterogeneous nucleation in the model. All equations that describe the evolution of temperature (T [K]), pressure (P [hPa]), the ice mass mixing ratio (q_i) and ice particle size (R_i [μm]) can be found in Pruppacher and Klett (1997). To conserve total water mass, the water vapor saturation ratio with respect to ice (S_i) is diagnosed from the total water conservation equation. The dry sulfate aerosol is assumed to follow a monodisperse size population, or a lognormal size distribution with an upper cutoff radius of 1 μm. The number of aerosol size bins (i.e., N_{bin}) varies from 1 (i.e., monodisperse) to 200. For a lognormal size distribution, each bin width is the same based on the logarithm of the particle size. The geometric dispersion (σ) of the dry sulfate aerosol size distribution which describes how spread out the sizes of aerosol populations are is an input parameter and has a value of 0 (i.e., monodisperse), 1.6 (Kärcher et al., 2006; Kärcher & Lohmann, 2002a), or 2.3 (Lin et al., 2002; Liu & Penner, 2005). The geometric mean dry sulfate aerosol size (R_a [μm]) is another input parameter, with a value of 0.02 or 0.2 μm. The homogeneous nucleation rate (J [m^{-3} s^{-1}]) is calculated based on water activity (Koop et al., 2000). The deposition coefficient (α_i) of water vapor on ice crystals is an input parameter, with a value of 0.1 as used in LP and BN or 0.5 as used in KL. To minimize the numerical diffusion, the ice crystal population formed from each aerosol size bin in each model time step is recorded using the particle tracking method, following Barahona and Nenes (2008). The updraft velocity (V [cm s^{-1}]) is constant. The initial model time step is 2 V^{-1} s and reduces to 0.05 V^{-1} s when nucleation occurs ($J > 10^4$ m^{-3} s^{-1}). The sedimentation of ice particles is also taken into account. The terminal fall velocity and the fraction of ice particles that fall out of the cloud parcel follow the method from Kay et al. (2006).

Table 1 lists the six model experiments conducted in this study. For each experiment, a variety of V (from 2 to 500 cm s^{-1}) and N_a (from 10 to 500 cm^{-3}) are used. The purpose of these experiments is to examine the

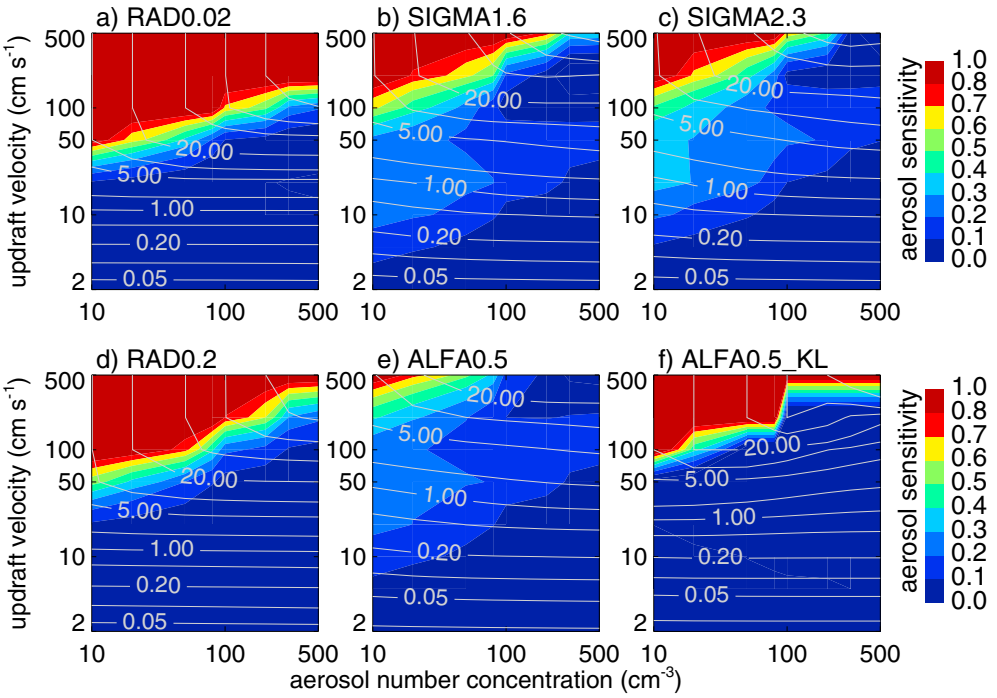

Figure 1. Ice crystals number concentration (N_i) contoured as a function of vertical velocity (V) and sulfate aerosol number concentration (N_a) from parcel model experiments. Colors indicate the values of the aerosol sensitivity parameter, η_α. Experiment names are shown in the upper-left corners.

sensitivity of η_α to aerosol size distributions (R_a and σ), the ice deposition coefficient (α_i), and an assumption made in the KL parameterization (defined below). Figure 1 shows the results of these experiments. In the RAD0.02 and RAD0.2 experiments, the sulfate aerosol size is monodispersed. For weak updrafts ($V < 50$ cm s^{-1}), the fraction of frozen sulfate aerosol particles (f_c) is less than 50%. At the maximum S_i during the parcel ascent, the increasing rate of S_i caused by the updraft velocity is balanced by the decreasing rate due to ice crystal growth. N_i depends mainly on V and is not sensitive to N_a. Thus, η_α is close to 0. This is also indicated by the flat contours of N_i with respect to N_a. For stronger updrafts ($V > 100$ cm s^{-1}), more aerosol particles are nucleated, and N_i is significantly sensitive to N_a. Therefore, η_α increases to appreciable values. Note that the ice growth rate is proportional to the ice crystal size (Shi et al., 2015). Compared to the RAD0.02 experiment, less ice crystals (i.e., a lower f_c) in RAD0.2 can cause S_i to decrease faster due to larger ice crystal sizes. This is why η_α from RAD0.2 is slightly smaller than that from RAD0.02 for a high V (>100 cm s^{-1}). We note that the pattern of η_α variations from RAD0.2 is very similar to that of Kay and Wood (2008), which also used a monodisperse aerosol distribution under the same thermodynamic conditions (T, P, α_i) and the same aerosol size (R_a) as the RAD0.2.

If sulfate aerosols follow a lognormal size distribution, as observed in the upper troposphere (Lin et al., 2002; Liu & Penner, 2005), aerosols in larger size bins will freeze earlier than aerosols in smaller size bins. At low V (<0.5 m s^{-1}), freshly nucleated ice crystals come mostly from larger aerosol size bins ($R > 0.1$ μm). Compared to the RAD0.02 experiment, N_i is lower in the SIGMA1.6 and SIGMA2.3 experiments due to the formation of larger ice crystals, which deplete water vapor in the cloud parcel. Although larger aerosol particles tend to freeze earlier and, thus, prohibit smaller aerosol particles from freezing, ice crystals can still be nucleated from aerosols in smaller size bins. The number of ice crystals depends on N_a (note the nonflat contours of changes in N_i with N_a in the SIGMA1.6 and SIGMA2.3 experiments). Thus, η_α values from SIGMA1.6 and SIGMA2.3 are significantly larger than those of RAD0.02 in weak updrafts ($V < 50$ cm s^{-1}). Furthermore, the comparison between SIGMA1.6 and SIGMA2.3 indicates that η_α increases with an increasing σ. N_i from ALFA0.5 is lower than that from SIGMA1.6 due to a larger α_i in ALFA0.5, resulting in the faster depletion of water vapor. Thus, increasing α_i in ALFA0.5 results in smaller η_α, compared to SIGMA1.6.

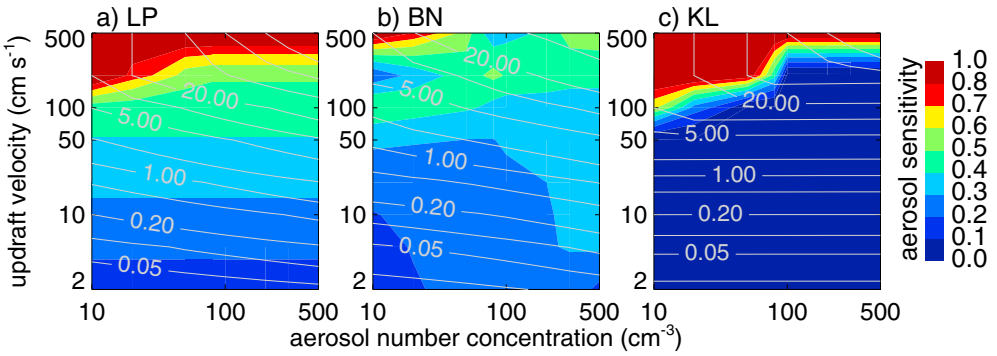

Figure 2. As in Figure 1, but for the results from (a) LP, (b) BN, and (c) KL ice nucleation parameterizations; T = 220 K and P = 250 hPa.

In the KL parameterization, aerosol particles freeze according to particle size. Aerosol particles in the largest size bin will freeze first when S_i reaches the homogeneous freezing threshold (S_{hom}). After that, aerosol particles in the second largest bin will freeze if the water vapor depletion rate (due to the deposition of water vapor on newly formed ice crystals from the largest bin) is less than the water vapor increasing rate, which is caused by the updraft velocity. Aerosol particles in the rest of size bins will nucleate chronologically until the water vapor depletion rate equals the water vapor increasing rate. Under this assumption, competition among different aerosol size bins is not allowed. In our ALFA0.5_KL experiment, the homogeneous freezing of aerosols in the parcel model is treated based on the same assumptions as in the KL parameterization. As seen in Figure 1, η_α from the ALFA0.5_KL is close to zero at $V < 50$ cm s^{-1}, which is very different from the ALFA0.5. Note that N_i slightly decreases with increasing N_a (i.e., $\eta_\alpha < 0$) in some regimes in the ALFA0.5_KL. The reason is that the size of nucleated ice crystals increases with increasing N_a. Larger ice crystals deplete water vapor faster and thus lower N_i. Note that in Figure 1 the color bar for $\eta_\alpha < 0$ uses the same one as for $\eta_\alpha = 0$.

3. Comparison of η_α Among Ice Nucleation Parameterizations

Here we compare the η_α calculated from the three ice nucleation parameterizations: LP, BN, and KL. We turn off the heterogeneous nucleation in these experiments. The LP parameterization is derived from fitting the simulation results of an adiabatically rising cloud parcel model with α_i = 0.1, σ = 2.3, and R_a = 0.02 μm. N_i is fitted as a function of relative humidity, T, V, and N_a. The BN parameterization is derived from the analytical solution from the cloud parcel equations. Variables α_i, σ, and R_a are input parameters with values of 0.1, 2.3, and 0.02 μm, respectively. The KL parameterization explicitly calculates the evolution of S_i in a rising cloud parcel. The variables α_i, σ, and R_a are input parameters, which are set to 0.5, 1.6, and 0.02 μm, respectively.

Figure 2 shows the η_α distribution as a function of N_a and V calculated from the three ice nucleation parameterizations. The η_α distribution pattern from LP is similar to BN in that η_α ranges from 0.1 to 0.3 at $V < 50$ cm s^{-1}, which is equivalent to an increase in N_i by a factor of 1.3–2.0 for a tenfold increase in N_a. The slopes of the N_i contours with respect to N_a are also quite similar. Both LP and BN parameterizations are developed based on their parcel model results with the same aerosol size distribution (i.e., R_a = 0.02 μm and σ = 2.3). Compared to the parcel model results under the same aerosol size distribution (R_a and σ) and α_i parameter (Figure 1, SIGMA2.3), the η_α values from LP and BN are slightly larger. We note that the η_α values from both the LP and BN parameterizations agree well with their corresponding parcel model results in most cases (Figure 2 of Liu & Penner, 2005 and Figure 9 of Barahona & Nenes, 2009). Thus, reasons for a larger η_α in LP and BN mainly come from differences among different parcel models. For example, in the parcel model used for LP, the nucleation rate J was calculated using the effective freezing temperature approach (Sassen & Dodd, 1988) rather than the water activity approach in this study (Koop et al., 2000). In the work of Barahona and Nenes (2009), N_{bin} is set to 20. Our parcel model testing shows that η_α with N_{bin} = 20 is higher than that of N_{bin} = 200 under the same conditions (not shown). In contrast, η_α from the KL parameterization is almost zero for a low V (Figure 2), which is significantly less than that from ALFA0.5 in Figure 1 and very similar to that from ALFA0.5_KL which uses the same assumption (discussed in section 2) as in the KL parameterization.

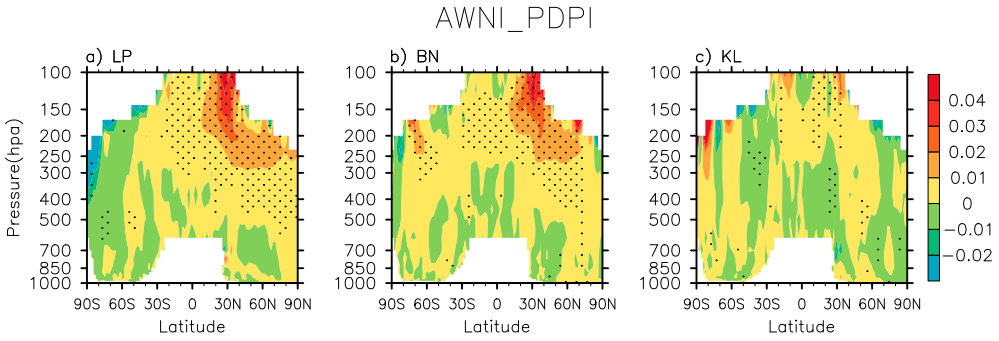

Figure 3. Changes (PD-PI) in annual zonal mean in-cloud ice crystal number concentrations (ΔN_i [cm^{-3}]) from model simulations with (a) LP, (b) BN, and (c) KL ice nucleation parameterizations. Differences significant at the 95% level of the Student's *t* test are depicted by dots.

4. Implications of η_α Differences for AIF

Here we study the implications of different η_α from ice nucleation parameterizations for ice AIF using a GCM (CAM5.1) (Neale et al., 2012). This model includes a two-moment stratiform cloud microphysics scheme (Gettelman et al., 2010; Morrison & Gettelman, 2008), coupled with a three-mode version of a modal aerosol module (Liu, Easter, et al., 2012) and enables the treatment of aerosol effects on both liquid and ice clouds. The ice nucleation process is represented by the LP parameterization. Coarse mode dust represents heterogeneous ice nucleating particles. Homogeneous nucleation uses sulfate aerosol particles in the Aitken mode. The subgrid scale variability of vertical velocity (W_{sub}), which is diagnosed from the square root of turbulent kinetic energy (Bretherton & Park, 2009), is used to drive the ice nucleation parameterization. A pair of PD (i.e., the year 2000) and PI (i.e., the year 1850) simulations is conducted to derive aerosol AIF. To isolate the anthropogenic AIF on cirrus clouds from that on liquid-phase clouds, the ice nucleation parameterization is driven by PD or PI aerosols prescribed from baseline model simulations, whereas the droplet activation parameterization for liquid clouds is driven by PD aerosols online calculated. Simulations are carried out at a horizontal resolution of 1.9° × 2.5°, with prescribed climatological sea surface temperatures and sea ice. Furthermore, we implement the BN and KL ice nucleation parameterizations in CAM5.1 (Shi et al., 2015) and compare simulations from LP, BN and KL ice nucleation parameterizations in the same CAM5.1 model. All simulations are run for a period of 11 years, and results from the last 10 years are used in the analysis.

Figure 3 shows changes (PD minus PI) in the annual zonal mean for in-cloud ice crystal number concentrations (ΔN_i [cm^{-3}]) from model simulations using the three ice nucleation parameterizations. ΔN_i from LP and BN is significant (>0.01 cm^{-3}) in the upper troposphere at midlatitudes over the Northern Hemisphere (NH), where sulfate N_a increases significantly from PI to PD (not shown). In contrast, ΔN_i from KL is not statistically significant. Table 2 gives global annual mean values of the cloud variables at PD and their changes (Δ) between PD and PI for the three ice nucleation parameterizations. The change in cloud droplet

Table 2
Global Annual Mean Cloud Variables at PD and Their Changes (Δ) Between PD and PI From the CAM5.1 Simulations for Three Ice Nucleation Parameterizations (LP, BN, and KL)

Parameterization	CF	LWCF	SWCF	IWP	LWP	CDNI
LP	−27.84	25.86	−53.70	19.19	45.32	1.50
BN	−27.81	25.46	−53.27	18.77	45.09	1.45
KL	−28.15	25.06	−53.21	18.77	45.20	1.50
ΔLP	0.13 ± 0.60	0.36 ± 0.72	−0.23 ± 0.87	0.20 ± 0.74	0.06 ± 0.97	0.09 ± 0.14
ΔBN	0.10 ± 0.61	0.33 ± 0.68	−0.23 ± 0.89	0.19 ± 0.70	0.08 ± 0.95	0.08 ± 0.11
ΔKL	−0.13 ± 0.64	0.05 ± 0.49	−0.18 ± 0.77	−0.01 ± 0.65	0.08 ± 1.00	0.03 ± 0.07

Note. Changes are shown for net cloud forcing (CF [W m^{-2}]), as well as the longwave (LWCF [W m^{-2}]) and shortwave (SWCF [W m^{-2}]) components, ice water path (IWP [g m^{-2}]), liquid water path (LWP [g m^{-2}]), and column cloud ice number concentration (CDNI [10^8 m^{-2}]). Standard deviations (±) are estimated from averages of each of 10 years.

number concentration is negligible because PD online aerosols are used in both PD and PI simulations (not shown). The change in the vertically integrated (i.e., column) cloud ice number concentration (ΔCDNI) from KL is 0.03×10^8 m^{-2}, which is much lower than those from LP (0.09×10^8 m^{-2}) and BN (0.08×10^8 m^{-2}). Correspondingly, the change in ice water path (ΔIWP) from KL (−0.01 g m^{-2}) is much smaller than that from LP (0.20 g m^{-2}) and BN (0.19 g m^{-2}). As a result, the change in longwave cloud forcing (ΔLWCF) from KL (0.05 W m^{-2}) is much weaker than that from LP (0.36 W m^{-2}) and BN (0.33 W m^{-2}). The shortwave cloud forcing (SWCF) is dominated by low-level warm clouds. Changes in cirrus cloud microphysics (e.g., increase in N_i) can lead to the increase of atmospheric stability and the weakening of convection (Andrews et al., 2010; Wang et al., 2014). Because of the weakening of convection, the large-scale cloud liquid water path (LWP) increases. ΔLWP from LP, BN, and KL experiments are 0.06, 0.08, and 0.08 g m^{-2}, respectively (Table 2). This is a major contribution to negative ΔSWCF. The ΔSWCF values from LP, BN, and KL are −0.23, −0.23, and −0.18 W m^{-2}, respectively. Although the negative ΔIWP for KL should lead to a positive change in SWCF of cirrus clouds, the overall ΔSWCF is negative for KL, due to the more negative change in SWCF of warm clouds. We note that ΔCF from KL is negative (−0.13 W m^{-2}), whereas ΔCF is positive for LP (0.13 W m^{-2}) and BN (0.10 W m^{-2}). However, these ΔCFs are generally within ±1 standard deviation.

5. Discussion and Summary

There are still large disagreements regarding the sensitivity of N_i that is formed from homogeneous nucleation in cirrus clouds to N_a (e.g., Barahona & Nenes, 2008, 2009; Jensen & Toon, 1994; Kärcher & Lohmann, 2002a, 2002b; Kärcher et al., 2006; Kay & Wood, 2008; Liu & Penner, 2005). To attribute the causes of these discrepancies, we run a cloud parcel model (Shi & Liu, 2016) for a variety of aerosol and thermodynamic conditions. The modeled aerosol sensitivity of η_α (i.e., the sensitivity of N_i to N_a) is close to zero at updrafts of $V < 50$ cm s^{-1}, which is very similar to that of Kay and Wood (2008) when a monodisperse aerosol size distribution is used. When we change the aerosol size distribution from monodisperse to a lognormal function typical of the upper troposphere, aerosol sensitivity is significantly increased. This may explain the very small aerosol sensitivity in Kay and Wood (2008), which assumed a monodisperse aerosol size distribution. Furthermore, η_α increases when the geometric dispersion of the aerosol size distribution (σ) is larger.

Differences in η_α among the three ice nucleation parameterizations (i.e., LP, BN, and KL) widely used in GCMs for studying aerosol effects on ice clouds are also investigated. At low V (<50 cm s^{-1}), N_i is moderately sensitive to N_a for LP and BN, whereas N_i is insensitive to N_a for KL; all three parameterizations use a similar lognormal aerosol size distribution. We find that the approach used in the KL parameterization, that is, aerosol particles freeze chronologically by aerosol size and therefore neglect the competition among different sizes of particles, results in extremely low sensitivity in the KL. If the same KL approach is used in our parcel model calculation, we can reproduce a nearly zero aerosol sensitivity, similar to KL.

The implications of η_α differences in these three parameterizations for ice cloud AIF are investigated with the CAM5.1. The anthropogenic longwave AIF ranges from 0.05 (KL) to 0.33 (BN) and 0.36 W m^{-2} (LP). This may explain why the longwave AIF is much stronger in the CAM5.1 (0.40–0.52 W m^{-2}) with the LP parameterization (Ghan et al., 2012) than that in the ECHAM-HAM2 (0.05–0.2 W m^{-2}) with the KL parameterization (Zhang et al., 2012).

This study suggests that a larger η_α (0.1–0.3) is more plausible and the homogeneous nucleation parameterizations should include a realistic aerosol size distribution to account for the competition of water vapor among different sizes of particles. By including the aerosol size distribution in the homogeneous nucleation parameterizations, this will contribute to the reduction of aerosol longwave indirect forcing spread in models. We note that this spread in models can result from other sources of uncertainties in the representation of cirrus clouds, for example, the occurrence frequency of homogeneous nucleation, which depends critically on subgrid vertical velocity (Shi & Liu, 2016). Current models show the dominant role of homogeneous nucleation versus heterogeneous nucleation in the formation of ice crystals, especially in tropical upper tropospheric cirrus (Shi et al., 2015; Zhou et al., 2016), contrary to the observations (Jensen et al., 2013). If homogeneous nucleation is deemed to occur less frequently, the longwave indirect forcing will be lower than those estimated in the CAM5.1 by LP and BN (Table 2). The aerosol longwave indirect forcing of 0.05 to 0.36 W m^{-2} estimated in this study is comparable (albeit smaller) in magnitude, but in the opposite sign

to the radiative forcing of −0.45 (−1.2 to 0.0) W m^{-2} due to aerosol-cloud interactions (Myhre et al., 2013). It can contribute to the warming from well-mixed greenhouse gases with a positive forcing of 2.83 (2.54 to 3.12) W m^{-2}. The aerosol indirect effects through cirrus clouds can lead to the increase of atmospheric stability, the weakening of convection, and the change of atmospheric humidity (Andrews et al., 2010; Liu et al., 2009; Wang et al., 2014) and thus can be an important driver of climate change in the twentieth century.

Acknowledgments
This research was supported by the National Science Foundation under grant ATM-1642289 and Climate Model Development and Validation Activity funded by the Office of Biological and Environmental Research in the U.S. Department of Energy Office of Science. X. Shi would also like to acknowledge the support from the National Natural Science Foundation of China (grant 41205071). We would like to acknowledge the use of computational resources (ark:/85065/d7wd3xhc) at the NCAR-Wyoming Supercomputing Center provided by the National Science Foundation and the State of Wyoming and supported by NCAR's Computational and Information Systems Laboratory. The CAM5 source code and input data sets are available at http://www2.cesm.ucar.edu.

References

Andrews, T., Forster, P. M., Boucher, O., Bellouin, N., & Jones, A. (2010). Precipitation, radiative forcing and global temperature change. *Geophysical Research Letters*, *37*, L14701. https://doi.org/10.1029/2010GL043991

Barahona, D., Molod, A., Bacmeister, J., Nenes, A., Gettelman, A., Morrison, H., et al. (2014). Development of two-moment cloud microphysics for liquid and ice within the NASA Goddard Earth Observing System Model (GEOS-5). *Geoscientific Model Development*, *7*(4), 1733–1766. https://doi.org/10.5194/gmd-7-1733-2014

Barahona, D., & Nenes, A. (2008). Parameterization of cirrus cloud formation in large-scale models: Homogeneous nucleation. *Journal of Geophysical Research*, *113*, D11211. https://doi.org/10.1029/2007JD009355

Barahona, D., & Nenes, A. (2009). Parameterizing the competition between homogeneous and heterogeneous freezing in ice cloud formation—Polydisperse ice nuclei. *Atmospheric Chemistry and Physics*, *9*(2), 369–381. https://doi.org/10.5194/acp-9-369-2009

Barahona, D., & Nenes, A. (2011). Dynamical states of low temperature cirrus. *Atmospheric Chemistry and Physics*, *11*(8), 3757–3771. https://doi.org/10.5194/acp-11-3757-2011

Boucher, O., Randall, D., Artaxo, P., Bretherton, C., Feingold, G., Forster, P., et al. (2013). Clouds and aerosols. In T. F. Stocker, et al. (Eds.), *Climate change 2013: The physical science basis. Contribution of Working Group I to the Fifth Assessment Report of the Intergovernmental Panel on Climate Change* (Chap. 7, pp. 571–657). Cambridge, United Kingdom and New York: Cambridge University Press.

Bretherton, C. S., & Park, S. (2009). A new moist turbulence parameterization in the Community Atmosphere Model. *Journal of Climate*, *22*(12), 3422–3448. https://doi.org/10.1175/2008jcli2556.1

Cziczo, D. J., Froyd, K. D., Hoose, C., Jensen, E. J., Diao, M., Zondlo, M. A., et al. (2013). Clarifying the dominant sources and mechanisms of cirrus cloud formation. *Science*, *340*(6138), 1320–1324. https://doi.org/10.1126/science.1234145

DeMott, P. J., Cziczo, D. J., Prenni, A. J., Murphy, D. M., Kreidenweis, S. M., Thomson, D. S., et al. (2003). Measurements of the concentration and composition of nuclei for cirrus formation. *Proceedings of the National Academy of Sciences of the United States of America*, *100*(25), 14,655–14,660. https://doi.org/10.1073/pnas.2532677100

Fan, J., Wang, Y., Rosenfeld, D., & Liu, X. (2016). Review of aerosol-cloud interactions: Mechanisms, significance and challenges. *Journal of the Atmospheric Sciences*, *73*(11), 4221–4252. https://doi.org/10.1175/JAS-D-16-0037.1

Gettelman, A., Liu, X., Ghan, S. J., Morrison, H., Park, S., Conley, A. J., et al. (2010). Global simulations of ice nucleation and ice supersaturation with an improved cloud scheme in the Community Atmosphere Model. *Journal of Geophysical Research*, *115*, D18216. https://doi.org/10.1029/2009JD013797

Ghan, S. J., Liu, X., Easter, R. C., Zaveri, R., Rasch, P. J., & Yoon, J.-H. (2012). Toward a minimal representation of aerosols in climate models: Comparative decomposition of aerosol direct, semidirect, and indirect radiative forcing. *Journal of Climate*, *25*, 6461–6476.

Jensen, E. J., Diskin, G., Lawson, R. P., Lance, S., Bui, T. P., Hlavka, D., et al. (2013). Ice nucleation and dehydration in the tropical tropopause layer. *Proceedings of the National Academy of Sciences of the United States of America*, *110*(6), 2041–2046. https://doi.org/10.1073/pnas.1217104110

Jensen, E. J., & Toon, O. B. (1994). Ice nucleation in the upper troposphere: Sensitivity to aerosol number density, temperature, and cooling rate. *Geophysical Research Letters*, *21*, 2019–2022.

Kärcher, B., Hendricks, J., & Lohmann, U. (2006). Physically based parameterization of cirrus cloud formation for use in global atmospheric models. *Journal of Geophysical Research*, *111*, D01205. https://doi.org/10.1029/2005JD006219

Kärcher, B., & Lohmann, U. (2002a). A parameterization of cirrus cloud formation: Homogeneous freezing of supercooled aerosols. *Journal of Geophysical Research*, *107*(D2), 4010. https://doi.org/10.1029/2001JD000470

Kärcher, B., & Lohmann, U. (2002b). A Parameterization of cirrus cloud formation: Homogeneous freezing including effects of aerosol size. *Journal of Geophysical Research*, *107*(D23), 4698. https://doi.org/10.1029/2001JD001429

Kay, J. E., Baker, M., & Hegg, D. (2006). Microphysical and dynamical controls on cirrus cloud optical depth distributions. *Journal of Geophysical Research*, *111*, D24205. https://doi.org/10.1029/2005JD006916

Kay, J. E., & Wood, R. (2008). Timescale analysis of aerosol sensitivity during homogeneous freezing and implications for upper tropospheric water vapor budgets. *Geophysical Research Letters*, *35*, L10809. https://doi.org/10.1029/2007GL032628

Koop, T., Luo, B. P., Tsias, A., & Peter, T. (2000). Water activity as the determinant for homogeneous ice nucleation in aqueous solutions. *Nature*, *406*(6796), 611–614. https://doi.org/10.1038/35020537

Kuebbeler, M., Lohmann, U., Hendricks, J., & Kärcher, B. (2014). Dust ice nuclei effects on cirrus clouds. *Atmospheric Chemistry and Physics*, *14*(6), 3027–3046. https://doi.org/10.5194/acp-14-3027-2014

Lin, R.-F., O'C Starr, D., DeMott, P., Cotton, R., Sassen, K., Jensen, E., et al. (2002). Cirrus parcel model comparison project phase 1: The critical components to simulate cirrus initiation explicitly. *Journal of the Atmospheric Sciences*, *59*(15), 2305–2329. https://doi.org/10.1175/1520-0469(2002)059%3C2305:CPMCPP%3E2.0.CO;2

Liu, X., Easter, R. C., Ghan, S. J., Zaveri, R., Rasch, P., Shi, X., et al. (2012). Toward a minimal representation of aerosols in climate models: Description and evaluation in the Community Atmosphere Model CAM5. *Geoscientific Model Development*, *5*(3), 709–739. https://doi.org/10.5194/gmd-5-709-2012

Liu, X., Penner, J. E., & Wang, M. (2009). Influence of anthropogenic sulfate and soot on upper tropospheric clouds using CAM3 coupled with an aerosol model. *Journal of Geophysical Research*, *114*, D03204. https://doi.org/10.1029/2008JD010492

Liu, X., Shi, X., Zhang, K., Jensen, E. J., Gettelman, A., Barahona, D., et al. (2012). Sensitivity studies of dust ice nuclei effect on cirrus clouds with the Community Atmosphere Model CAM5. *Atmospheric Chemistry and Physics*, *12*(24), 12,061–12,079. https://doi.org/10.5194/acp-12-12061-2012

Liu, X. H., & Penner, J. E. (2005). Ice nucleation parameterization for global models. *Meteorologische Zeitschrift*, *14*(4), 499–514. https://doi.org/10.1127/0941-2948/2005/0059

Lohmann, U., & Feichter, J. (2005). Global indirect aerosol effects: A review. *Atmospheric Chemistry and Physics*, *5*(3), 715–737. https://doi.org/10.5194/acp-5-715-2005

Morrison, H., & Gettelman, A. (2008). A new two-moment bulk stratiform cloud microphysics scheme in the Community Atmosphere Model, version 3 (CAM3). Part I: Description and numerical tests. *Journal of Climate*, *21*(15), 3642–3659. https://doi.org/10.1175/2008jcli2105.1

Murray, B. J., Wilson, T. W., Dobbie, S., Cui, Z., al-Jumur, S. M. R. K., Möhler, O., et al. (2010). Heterogeneous nucleation of ice particles on glassy aerosols under cirrus conditions. *Nature Geoscience*, *3*(4), 233–237. https://doi.org/10.1038/ngeo817

Myhre, G., Shindell, D., Bréon, F.-M., Collins, W., Fuglestvedt, J., Huang, J., et al. (2013). Anthropogenic and natural radiative forcing. In T. F. Stocker, et al. (Eds.), *Climate change 2013: The physical science basis. Contribution of Working Group I to the Fifth Assessment Report of the Intergovernmental Panel on Climate Change* (pp. 659–740). Cambridge, UK: Cambridge University Press.

Neale, R. B., Gettelman, A., Park, S., Conley, A. J., Kinnison, D., Marsh, D., et al. (2012). Description of the NCAR Community Atmosphere Model (CAM 5.0), NCAR Tech. Note NCAR/TN-485+STR (289 pp.). Boulder, CO: National Center for Atmospheric Research.

Pruppacher, H. R., & Klett, J. D. (1997). *Microphysics of cloud and precipitation* (p. 954). New York: Springer.

Sassen, K., & Dodd, G. C. (1988). Homogeneous nucleation rate for highly supercooled cirrus cloud droplets. *Journal of the Atmospheric Sciences*, *45*(8), 1357–1369. https://doi.org/10.1175/1520-0469(1988)045%3C1357:HNRFHS%3E2.0.CO;2

Shi, X., & Liu, X. (2016). Effect of cloud-scale vertical velocity on the contribution of homogeneous nucleation to cirrus formation and radiative forcing. *Geophysical Research Letters*, *43*, 6588–6595. https://doi.org/10.1002/2016GL069531

Shi, X., Liu, X., & Zhang, K. (2015). Effects of preexisting ice crystals on cirrus clouds and comparison between different ice nucleation parameterizations with the Community Atmosphere Model (CAM5). *Atmospheric Chemistry and Physics*, *15*(3), 1503–1520. https://doi.org/10.5194/acp-15-1503-2015

Twomey, S. A. (1977). The influence of pollution on the shortwave albedo of clouds. *Journal of the Atmospheric Sciences*, *34*, 1149–1152. https://doi.org/10.1175/1520-0469(1977)034%3C1149:TIOPOT%3E2.0.CO;2

Wang, M., Liu, X., Zhang, K., & Comstock, J. M. (2014). Aerosol effects on cirrus through ice nucleation in the Community Atmosphere Model CAM5 with a statistical cirrus scheme. *Journal of Advances in Modeling Earth Systems*, *6*(3), 756–776. https://doi.org/10.1002/2014MS000339

Zhang, K., Liu, X., Wang, M., Comstock, J. M., Mitchell, D. L., Mishra, S., & Mace, G. G. (2013). Evaluating and constraining ice cloud parameterizations in CAM5 using aircraft measurements from the SPARTICUS campaign. *Atmospheric Chemistry and Physics*, *13*(9), 4963–4982. https://doi.org/10.5194/acp-13-4963-2013

Zhang, K., O'Donnell, D., Kazil, J., Stier, P., Kinne, S., Lohmann, U., et al. (2012). The global aerosol-climate model ECHAM-HAM, version 2: sensitivity to improvements in process representations. *Atmospheric Chemistry and Physics*, *12*, 8911–8949. https://doi.org/10.5194/acp-12-8911-2012

Zhou, C., Penner, J. E., Lin, G., Liu, X., & Wang, M. (2016). What controls the low ice number concentration in the upper troposphere? *Atmospheric Chemistry and Physics*, *16*(19), 12,411–12,424. https://doi.org/10.5194/acp-16-12411-2016